Ozone-CO correlations determined by the TES satellite instrument in continental outflow regions

Lin Zhang,[1] Daniel J. Jacob,[1] Kevin W. Bowman,[2] Jennifer A. Logan,[1]
Solène Turquety,[1,3] Rynda C. Hudman,[1] Qinbin Li,[2] Reinhard Beer,[2] Helen M. Worden,[2]
John R. Worden,[2] Curtis P. Rinsland,[4] Susan S. Kulawik,[2] Michael C. Lampel,[5]
Mark W. Shephard,[6] Brendan M. Fisher,[2] Annmarie Eldering,[2] and Melody A. Avery[7]

Received 23 March 2006; revised 6 July 2006; accepted 17 August 2006; published 21 September 2006.

[1] Collocated measurements of tropospheric ozone (O_3) and carbon monoxide (CO) from the Tropospheric Emission Spectrometer (TES) aboard the EOS Aura satellite provide information on O_3-CO correlations to test our understanding of global anthropogenic influence on O_3. We examine the global distribution of TES O_3-CO correlations in the middle troposphere (618 hPa) for July 2005 and compare to correlations generated with the GEOS-Chem chemical transport model and with ICARTT aircraft observations over the eastern United States (July 2004). The TES data show significant O_3-CO correlations downwind of polluted continents, with dO_3/dCO enhancement ratios in the range 0.4–1.0 mol mol^{-1} and consistent with ICARTT data. The GEOS-Chem model reproduces the O_3-CO enhancement ratios observed in continental outflow, but model correlations are stronger and more extensive. We show that the discrepancy can be explained by spectral measurement errors in the TES data. These errors will decrease in future data releases, which should enable TES to provide better information on O_3-CO correlations. **Citation:** Zhang, L., et al. (2006), Ozone-CO correlations determined by the TES satellite instrument in continental outflow regions, *Geophys. Res. Lett.*, *33*, L18804, doi:10.1029/2006GL026399.

1. Introduction

[2] The Tropospheric Emission Spectrometer (TES) launched aboard the Aura satellite in July 2004 measures global distributions of tropospheric ozone (O_3) together with carbon monoxide (CO) by IR emission [*Beer*, 2006]. The resulting information on O_3-CO correlations offers a test of current understanding of continental outflow and intercontinental transport of O_3 pollution. O_3 in the troposphere is produced by photochemical oxidation of CO and volatile organic compounds (VOCs) in the presence of nitrogen oxides ($NO_x \equiv NO + NO_2$). CO is a precursor of O_3 and a long-lived tracer of combustion. Observed O_3-CO correlations at continental outflow sites and from aircraft have been used in many studies to estimate the efficiency of O_3 formation and export [*Parrish et al.*, 1993, 1998; *Honrath et al.*, 2004]. Although simple quantitative interpretation in terms of O_3 production is complicated by sampling of air masses with varying background mixing ratios [*Chin et al.*, 1994; *Mauzerall et al.*, 1998], the correlation still provides a valuable test of model predictions of global anthropogenic influence on O_3 [*Chin et al.*, 1994; *Mauzerall et al.*, 2000; *Li et al.*, 2002]. We examine here the O_3-CO correlations observed by TES in July 2005 and compare them to results from a global 3-D tropospheric chemistry model (GEOS-Chem).

2. TES Observations and GEOS-Chem Simulation

[3] TES is a Fourier transform IR emission spectrometer with high spectral resolution (0.1 cm^{-1}) and a wide spectral range (650–3050 cm^{-1}) [*Beer et al.*, 2001]. The Aura satellite is on a polar Sun-synchronous orbit with equator crossing at 0145 and 1345 local time. TES standard products ("global surveys") consist of 16 orbits of nadir vertical profiles with 5 × 8 km^2 horizontal resolution spaced 1.6° along the orbit track. The retrievals have 1–2 degrees of freedom for signal (DOFS) for O_3 in the troposphere, and about 1 DOFS for CO. We use the V001 Beta Release data available at the Langley Atmospheric Science Data Center (ASDC). Comparisons of TES O_3 with ozonesonde data are presented by H. Worden et al. (Comparisons of Tropospheric Emission Spectrometer (TES) ozone profiles to ozonesondes: Methods and initial results, submitted to *Journal of Geophysical Research*, 2006). For V001 data, TES O_3 profiles agree well with ozonesondes up to 300 hPa but have a positive bias of up to 30 ppbv at higher latitudes in the upper troposphere. Comparisons of TES and MOPITT CO measurements show that TES has a 1%–6% negative bias relative to MOPITT (M. Luo et al., The influences of a priori data and instrument characteristics on nadir atmospheric species retrievals-Comparison of CO retrievals from TES and MOPITT, manuscript in preparation, 2006), but MOPITT has a 5% mean positive bias against in situ validation profiles [*Jacob et al.*, 2003; *Emmons et al.*, 2004]. We use O_3 and CO retrievals for July 2005 (14 global surveys) when large O_3 pollution enhancements over northern mid-latitudes are

[1]Department of Earth and Planetary Sciences and Division of Engineering and Applied Sciences, Harvard University, Cambridge, Massachusetts, USA.
[2]Jet Propulsion Laboratory, California Institute of Technology, Pasadena, California, USA.
[3]Now at Service d'Aéronomie, Institute Pierre-Simon Laplace, Université Pierre et Marie Curie, Paris, France.
[4]NASA Langley Research Center, Hampton, Virginia, USA.
[5]Raytheon Information Solutions, Pasadena, California, USA.
[6]Atmospheric and Environmental Research (AER), Inc., Lexington, Massachusetts, USA.
[7]Chemistry and Dynamics Branch, NASA Langley Research Center, Hampton, Virginia, USA.

0094-8276/06/2006GL026399

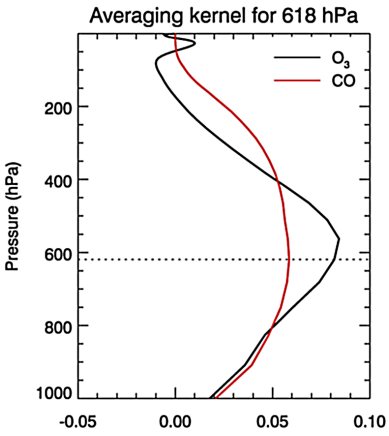

Figure 1. Sample averaging kernels for TES nadir retrievals of O_3 and CO at the 618 hPa level (23°N, 78°W from the global survey on 4–5 July 2005). The averaging kernels are applied to the logarithms of the mixing ratios [*Bowman et al.*, 2006].

expected. We exclude latitudes >60° where TES measurements are less reliable due to low brightness temperatures.

[4] The TES retrieval determines vertical profiles of logarithms of mixing ratios from the observed radiances using the optimal estimation method [*Rodgers*, 2000; *Bowman et al.*, 2006]. The retrieved mixing ratio profile $\hat{\mathbf{x}}$ can be expressed as:

$$\ln \hat{\mathbf{x}} = \ln \mathbf{x_a} + \mathbf{A}(\ln \mathbf{x} - \ln \mathbf{x_a}) + \varepsilon \quad (1)$$

where $\mathbf{x}$ is the true profile, $\mathbf{x_a}$ is the a priori constraint from monthly mean profiles simulated with the MOZART model [*Brasseur et al.*, 1998] and averaged over a 10° latitude × 60° longitude grid [*Bowman et al.*, 2006], $\mathbf{A}$ is the averaging kernel, and ε is the spectral measurement error with covariance matrix $\mathbf{S}_\varepsilon$. TES averaging kernels and spectral measurement errors are reported for each retrieved profile as part of the TES data set. We focus our analysis on the 618 hPa retrieval level where TES has good sensitivity for both O_3 and CO centered in the middle troposphere, with little influence from the stratosphere. Figure 1 shows typical TES averaging kernels at the 618 hPa level for O_3 and CO, describing the response of the retrieval at 618 hPa to a perturbation in the true profile at different pressure levels. Both kernels display broad peaks centered at the same altitude. We filter out retrievals with poor information (diagonal term of the averaging kernel <0.02).

[5] The GEOS-Chem global 3-D model for tropospheric chemistry was originally described by *Bey et al.* [2001]. We conduct a simulation for July 2005 using GEOS-Chem v7.02.04 (http:///www-as.harvard.edu/chemistry/trop/geos) driven by GEOS-4 assimilated meteorological observations from the NASA Global Modeling and Assimilation Office (GMAO). The GEOS-4 dataset has a temporal resolution of 6 hours (3 hours for surface variables and mixing depths), a horizontal resolution of 1° × 1.25°, and 55 layers in the vertical. We degrade the horizontal resolution to 2° × 2.5° for input to GEOS-Chem. Fire emissions are from a climatological biomass burning inventory [*Lobert et al.*, 1999; *Duncan et al.*, 2003] and are allocated daily on the basis of MODIS fire counts for July 2005. The GMAO meteorological data have excessive stratosphere-troposphere exchange (STE) [*Tan et al.*, 2004], hence we use the Synoz O_3 flux boundary condition at the tropopause [*McLinden et al.*, 2000]. General evaluations of the GEOS-Chem tropospheric O_3 simulation have been presented by *Bey et al.* [2001], *Martin et al.* [2002], *Liu et al.* [2006], and S. Wu et al. (Why are there large differences between models in global budgets of tropospheric ozone, submitted to *Journal of Geophysical Research*, 2006). Evaluations of continental outflow and intercontinental transport at mid-latitudes for O_3 and CO have been presented by *Li et al.* [2002, 2005], *Heald et al.* [2003], *Jaeglé et al.* [2003], and *Liang et al.* [2004].

[6] Model profiles are sampled along the TES orbit track at the observation time, and interpolated to the TES pressure grid as logarithms of mixing ratios. The coincidence is not perfect since the model has a 2° × 2.5° horizontal resolution (whereas observations are for a 5 × 8 km^2 scene) and model output is sampled every 3 hours (resulting in temporal offset with observations by up to 1.5 hours); the associated representation error is about 5% [*Heald et al.*, 2004]. To compare GEOS-Chem with the TES retrieved profiles, we must simulate the retrieval by applying the local averaging kernel. Since GEOS-Chem has no predictive capability in the stratosphere, we replace the simulated profiles above the model tropopause with the TES retrievals. The resulting profiles are then vertically smoothed with the TES averaging kernels according to equation (1). The measurement noise is assumed to be zero as the most likely value, so that the ε term is ignored; we will return to this point later.

[7] The geographically variable a priori used in the standard TES product helps to regularize the retrieval, but it also contributes structure to the retrieval that is not actually measured. To remove this artifact, we reprocess the TES profiles using a universal a priori:

$$\ln \hat{\mathbf{x}}' = \ln \hat{\mathbf{x}} + (\mathbf{I} - \mathbf{A})(\ln \mathbf{x'_a} - \ln \mathbf{x_a}) \quad (2)$$

where $\mathbf{x'_a}$ is the universal a priori obtained by averaging the original TES a priori constraint $\mathbf{x_a}$ in the 60°N–60°S band, and $\mathbf{I}$ is the identity matrix. The same correction is applied to the model fields. Figure 2 shows the reprocessed O_3 and CO concentrations at 618 hPa observed by TES for July 2005, and the corresponding concentrations simulated by GEOS-Chem. Both TES and GEOS-Chem show high values over polluted regions of northern mid-latitudes and biomass burning regions of Africa. Both show a Middle East O_3 maximum, whose origin was discussed by *Li et al.* [2001].

3. Global Distribution of O_3-CO Correlations

[8] We determined O_3-CO correlations in the TES data by binning the reprocessed observations for July 2005 into 10° × 10° grid cells. Each cell has 20–60 observations from which to derive the correlation. O_3-CO linear regressions for these reprocessed fields are obtained with the reduced major axis (RMA) method that allows for error in both variables [*Hirsch and Gilroy*, 1984]. The slope of the regression line represents the O_3-CO enhancement ratio (dO_3/dCO).

[9] Figure 3 (left) shows TES and GEOS-Chem O_3-CO scatterplots for a 10° × 10° gridbox over the eastern United States where TES observes a strong correlation due to North American outflow to the free troposphere. TES O_3 and CO

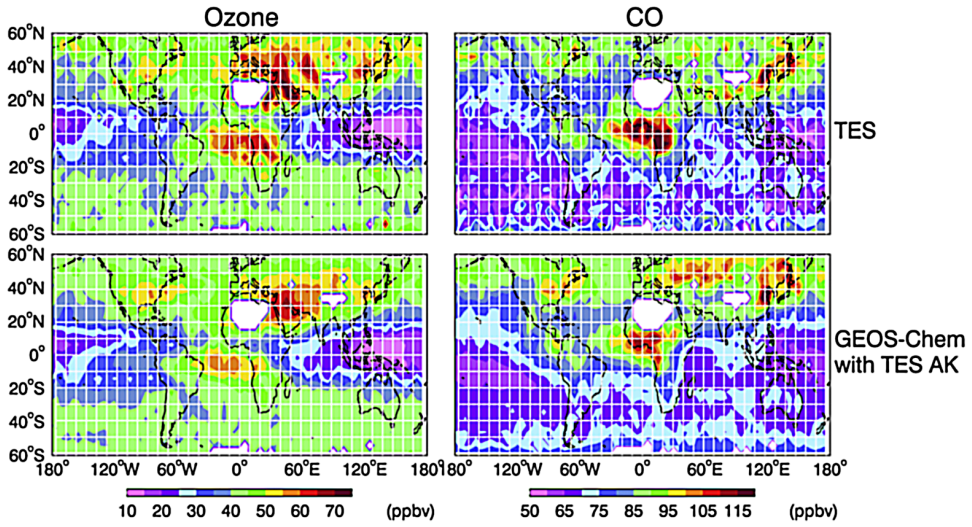

Figure 2. Mean concentrations of O_3 and CO at 618 hPa observed by TES for 4–31 July 2005, and corresponding GEOS-Chem model values sampled along the TES orbit tracks and with TES averaging kernels applied. The original TES data have been reprocessed following equation (2) to remove the effect of variable a priori, and averaged on a 4° × 5° grid with 5–15 data points in each grid square. White areas have no data meeting the retrieval quality criteria [*Osterman et al.*, 2005]. White lines indicate the 10° × 10° grid used to derive the O_3-CO correlations in Section 3.

are positively correlated (R = 0.5) with dO_3/dCO = 0.81 mol mol^{-1}. This enhancement ratio is larger than summertime observations of 0.2–0.5 mol mol^{-1} at surface sites in eastern North America [*Parrish et al.*, 1993; *Chin et al.*, 1994], but consistent with the mean observation of 1.0 mol mol^{-1} in free tropospheric North American outflow sampled at a mountaintop site in the Azores [*Honrath et al.*, 2004]. A higher dO_3/dCO relative to surface air is expected due to near-field ozone production in the free troposphere from exported NO_y [*Li et al.*, 2004], and has been observed previously for biomass burning plumes over aging times of about a week [*Mauzerall et al.*, 1998]. The model in Figure 3 shows a stronger correlation than TES (R = 0.70) but similar dO_3/dCO (0.63 mol mol^{-1}). Previous comparison of GEOS-Chem results with surface air observations at a Canadian maritime site (Sable Island) showed dO_3/dCO = 0.3 mol mol^{-1} in July, in good agreement with local observations [*Li et al.*, 2002].

[10] We also show in Figure 3 the observed in situ O_3-CO correlations over the same 10° × 10° domain at 600–650 hPa from the ICARTT aircraft campaign that took place in July–August 2004 over eastern North America. The correlation coefficient (R = 0.34) and enhancement ratio (dO_3/dCO = 0.72 mol mol^{-1}) for the 1-minute aircraft data are similar to the TES observations. We further include in Figure 3 the GEOS-Chem model results for ICARTT sampled along the aircraft flight tracks and for the flight days (R. C. Hudman et al., Characterization of North American ozone-CO correlations during the ICARTT study, manuscript in preparation, 2006). The simulated correlation (R = 0.44) and enhancement ratio (dO_3/dCO = 0.92 mol mol^{-1}) are similar to observed values.

[11] Figure 4 shows the global distribution of O_3-CO correlation coefficients and dO_3/dCO enhancement ratios in the TES data for July 2005. Significant positive correlations (R > 0.4) are observed downwind of the eastern United States and East Asia, and over central Africa. These three regions are known to have strong production and export of O_3 pollution in northern hemispheric summer [*Parrish et al.*, 1993; *Mauzerall et al.*, 1998, 2000]. The associated dO_3/dCO enhancement ratios are in the 0.4–1.0 mol mol^{-1} range. The

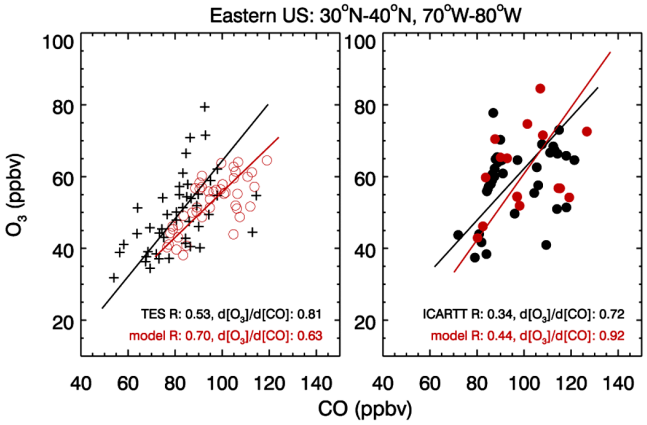

Figure 3. O_3-CO relationship in free tropospheric continental outflow over the eastern United States (30°–40°N, 70°–80°W) in July. (left) TES observations for July 2005 at 618 hPa reprocessed with equation (2) (black crosses) and corresponding model values from GEOS-Chem (red circles). (right) One-minute averaged aircraft observations (in black) at 600–650 hPa from the ICARTT campaign (July 3–August 15 2004), and corresponding GEOS-Chem model values sampled along the flight tracks (in red). The ICARTT measurements are from two aircraft, the NASA DC-8 and the NOAA WP-3D. There are 36 1-minute observations for the 10° × 10° domain and 600–650 hPa altitude range, and 15 corresponding model points sampled on the 2° × 2.5° model grid. Correlation coefficients (R) and slopes of the reduced-major-axis regression lines (dO_3/dCO, mol mol^{-1}) are shown inset.

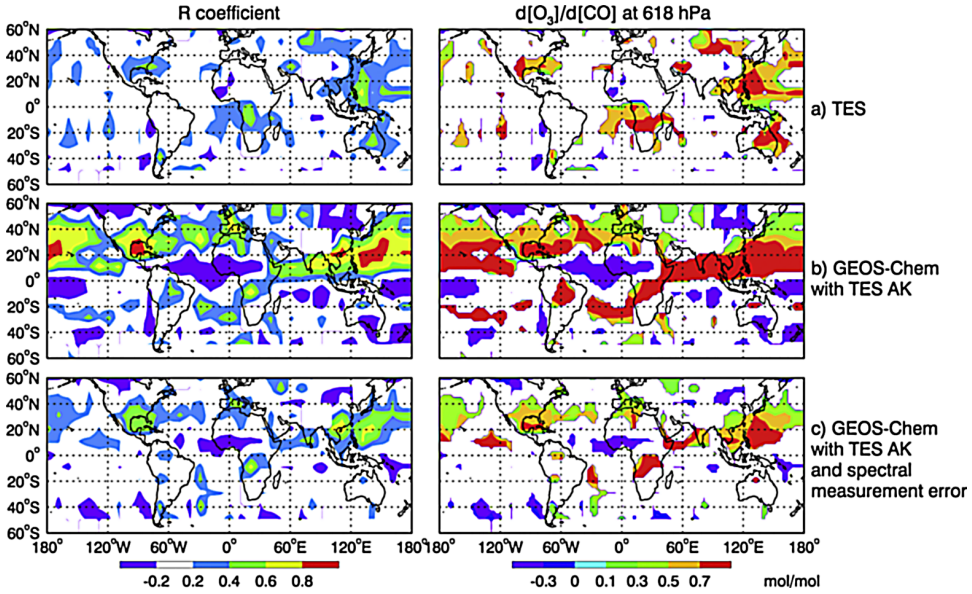

Figure 4. O_3-CO correlations for July 2005 at 618 hPa from (a) TES, (b) GEOS-Chem with TES averaging kernels (**A**) applied, and (c) GEOS-Chem with both TES averaging kernels and spectral measurement errors (ε) applied. The figure shows the correlation coefficients R and the linear regression slopes dO_3/dCO determined by the reduced major axis method. The data are computed in $10^\circ \times 10^\circ$ grid cells, and interpolated in the plot. White regions correspond to $|R| < 0.2$.

values of 0.6–0.8 mol mol^{-1} over Africa are consistent with the mean value of 0.7 mol mol^{-1} in old biomass burning plumes sampled during the TRACE-A aircraft campaign [*Mauzerall et al.*, 1998]. GEOS-Chem shows positive O_3-CO correlations over the same regions as TES but with stronger correlation coefficients and extending further downwind of the continents, displaying a pollution transport belt at northern mid-latitudes (Figure 4b). Weak negative correlations are found in remote regions where O_3 is delivered mainly by subsidence.

4. Effect of Retrieval Error

[12] We find that the stronger O_3-CO correlations in GEOS-Chem relative to TES at northern mid-latitudes can be explained by spectral measurement error in the TES data. This error, ε in equation (1), is typically 5–15% of the retrieved concentrations. Following standard practice, we did not apply it to the model fields in comparing simulated concentrations to satellite observations (Figure 2) since its expected value is the null vector and its effect becomes negligible when monthly average concentrations are considered. However, it increases the variance of the observations and hence degrades the O_3-CO correlations. We demonstrate this here by applying a realization of the random spectral measurement error to each model vertical profile used for the correlation analysis, assuming a normal distribution probability for ε and no correlation between the errors in the O_3 and CO spectral bands (the retrievals are done in different spectral windows [*Worden et al.*, 2004]). The resulting simulated O_3-CO correlations show values for R and dO_3/dCO that are in good agreement with the values observed by TES, in terms of both magnitudes and patterns (Figure 4c).

[13] We can also add spectral errors to the model fields analytically with some reasonable assumptions. Equation (1) can be written as $\ln \hat{\mathbf{x}} = \ln \mathbf{x}' + \varepsilon$, where $\mathbf{x}'$ is the retrieved profile under noise-free conditions. Assuming that spectral measurement errors are small in the conversion from log mixing ratio to mixing ratio, and that the spectral measurement error covariance $\mathbf{S}_\varepsilon$ is the same for all scenes, it can be shown that the correlation between any two elements $\hat{x}_i = [\hat{\mathbf{x}}]_i$ and $\hat{x}_j = [\hat{\mathbf{x}}]_j$ of the retrieved O_3 and CO profiles is

$$Corr(\hat{x}_i \hat{x}_j) = \frac{Cov\left(x'_i x'_j\right)}{\sqrt{s^2_{x'_i} + \overline{x'_i}^2 [\mathbf{S}_\varepsilon]_{ii}}\sqrt{s^2_{x'_j} + \overline{x'_j}^2 [\mathbf{S}_\varepsilon]_{jj}}} \quad (3)$$

where $Cov(\,)$ is the covariance, $\overline{x'_i}$ and $\overline{x'_j}$ are the mean values, and $\sigma_{x'i}$ and $\sigma_{x'j}$ are the standard deviations. The reduction in correlation due to spectral errors is evident from the expression. Results from this approach (not shown) are similar to those in Figure 4c.

5. Conclusions

[14] We have shown that correlations of concurrent tropospheric O_3 and CO measurements from space by the TES instrument provide valuable global information to test model estimates of anthropogenic influence on O_3. Positive O_3-CO correlation observed by TES in the free troposphere over the eastern United States in July 2005 is consistent with observations from the ICARTT aircraft campaign (July 2004) in terms of both correlation coefficient (R) and enhancement ratio (dO_3/dCO). Global distributions of O_3-CO correlations observed by TES for July 2005 are consistent with those derived from a global 3-D model of tropospheric chemistry (GEOS-Chem) and yield similar dO_3/dCO enhancement ratios in continental outflow regions. However, the model correlations are stronger and more extensive. We show that this can be explained by spectral measurement error in the TES V001 data, degrading the observed O_3-CO correlations.

The most recent TES V002 data have lower spectral measurement error due to improved radiance calibration [*Sarkissian et al.*, 2005] and warm-up of the TES optical bench (C. P. Rinsland et al., Nadir Measurements of Carbon Monoxide (CO) Distributions by the Tropospheric Emission Spectrometer Instrument onboard the Aura Spacecraft: Overview of Analysis Approach and Examples of Initial Results, submitted to *Geophysical Research Letters*, 2006). The next release V003 should further reduce the error by improvements of the TES temperature and cloud retrievals.

[15] **Acknowledgments.** This work was funded by the NASA EOS Program and by the NASA Atmospheric Composition Modeling and Analysis Program (ACMAP). We thank David Parrish, Tom Ryerson, and John Holloway for providing the NOAA WP-3D O_3 and CO data sets. We thank Glen Sachse for providing the NASA DC-8 CO measurements. We acknowledge useful comments from the two anonymous reviewers.

References

Beer, R. (2006), TES on the Aura Mission: Scientific objectives, measurements and analysis overview, *IEEE Trans. Geosci. Remote. Sens.*, *44*, 1102–1105.

Beer, R., T. A. Glavich, and D. M. Rider (2001), Tropospheric emission spectrometer for the Earth Observing System's Aura satellite, *Appl. Opt.*, *40*, 2356–2367.

Bey, I., D. J. Jacob, R. M. Yantosca, J. A. Logan, B. D. Field, A. M. Fiore, Q. Li, H. Liu, L. J. Mickley, and M. G. Schultz (2001), Global modeling of tropospheric chemistry with assimilated meteorology: Model description and evaluation, *J. Geophys. Res.*, *106*, 23,073–23,089.

Bowman, K. W., et al. (2006), Tropospheric emission spectrometer: Retrieval method and error analysis, *IEEE Trans. Geosci. Remote. Sens.*, *44*, 1297–1307.

Brasseur, G. P., D. A. Hauglustaine, S. Walters, P. J. Rasch, J.-F. Müller, C. Granier, and X. X. Tie (1998), MOZART: A global chemical transport model for ozone and related chemical tracers: 1. Model description, *J. Geophys. Res.*, *103*, 28,265–28,289.

Chin, M., D. J. Jacob, J. W. Munger, D. D. Parrish, and B. G. Doddridge (1994), Relationship of ozone and carbon monoxide over North America, *J. Geophys. Res.*, *99*, 14,565–14,573.

Duncan, B. N., R. V. Martin, A. C. Staudt, R. Yevich, and J. A. Logan (2003), Interannual and seasonal variability of biomass burning emissions constrained by satellite observations, *J. Geophys. Res.*, *108*(D2), 4100, doi:10.1029/2002JD002378.

Emmons, L. K., et al. (2004), Validation of Measurements of Pollution in the Troposphere (MOPITT) CO retrievals with aircraft in situ profiles, *J. Geophys. Res.*, *109*, D03309, doi:10.1029/2003JD004101.

Heald, C. L., et al. (2003), Asian outflow and transpacific transport of carbon monoxide and ozone pollution: An integrated satellite, aircraft and model perspective, *J. Geophys. Res.*, *108*(D24), 4804, doi:10.1029/2003JD003507.

Heald, C. L., D. J. Jacob, D. B. A. Jones, P. I. Palmer, J. A. Logan, D. G. Streets, G. W. Sachse, J. C. Gille, R. N. Hoffman, and T. Nehrkorn (2004), Comparative inverse analysis of satellite (MOPITT) and aircraft (TRACE-P) observations to estimate Asian sources of carbon monoxide, *J. Geophys. Res.*, *109*, D23306, doi:10.1029/2004JD005185.

Hirsch, R. M., and E. J. Gilroy (1984), Methods of fitting a straight line to data: Examples in water resources, *Water Resour. Bull.*, *20*, 705–711.

Honrath, R. E., R. C. Owen, M. Val Martacute;n, J. S. Reid, K. Lapina, P. Fialho, M. P. Dziobak, J. Kleissl, and D. L. Westphal (2004), Regional and hemisphere impacts of anthropogenic and biomass burning emissions on summertime CO and O_3 in the North Atlantic lower free troposphere, *J. Geophys. Res.*, *109*, D24310, doi:10.1029/2004JD005147.

Jacob, D. J., J. H. Crawford, M. M. Kleb, V. S. Connors, R. J. Bendura, J. L. Raper, G. W. Sachse, J. C. Gille, L. Emmons, and C. L. Heald (2003), The Transport and Chemical Evolution over the Pacific (TRACE-P) aircraft mission: Design, execution, and first results, *J. Geophys. Res.*, *108*(D4), 9000, doi:10.1029/2002JD003276.

Jaeglé, L., D. A. Jaffe, H. U. Price, P. Weiss-Penzias, P. I. Palmer, M. J. Evans, D. J. Jacob, and I. Bey (2003), Sources and budgets for CO and O_3 in the northeastern Pacific during the spring of 2001: Results from the PHOBEA-II Experiment, *J. Geophys. Res.*, *108*(D20), 8802, doi:10.1029/2002JD003121.

Li, Q., D. J. Jacob, J. A. Logan, I. Bey, R. M. Yantosca, H. Liu, R. V. Martin, A. M. Fiore, B. D. Field, B. N. Duncan, and V. Thouret (2001), A tropospheric ozone maximum over the Middle East, *Geophys. Res. Lett.*, *28*, 3235–3238.

Li, Q., et al. (2002), Transatlantic transport of pollution and its effects on surface ozone in Europe and North America, *J. Geophys. Res.*, *107*(D13), 4166, doi:10.1029/2001JD001422.

Li, Q., J. Jacob, J. W. Munger, R. M. Yantosca, and D. D. Parrish (2004), Export of NO_y from the North American boundary layer: Reconciling aircraft observations and global model budgets, *J. Geophys. Res.*, *109*, D02313, doi:10.1029/2003JD004086.

Li, Q., D. J. Jacob, R. Park, Y. Wang, C. L. Heald, R. Hudman, R. M. Yantosca, R. V. Martin, and M. Evans (2005), North American pollution outflow and the trapping of convectively lifted pollution by upper-level anticyclone, *J. Geophys. Res.*, *110*, D10301, doi:10.1029/2004JD005039.

Liang, Q., L. Jaeglé, D. A. Jaffe, P. Weiss-Penzias, A. Heckman, and J. A. Snow (2004), Long-range transport of Asian pollution to the Northeast Pacific: Seasonal variations and transport pathways of carbon monoxide, *J. Geophys. Res.*, *109*, D23S07, doi:10.1029/2003JD004402.

Liu, X., et al. (2006), First directly-retrieved global distribution of tropospheric column ozone: comparison with the GOES-CHEM model, *J. Geophys. Res.*, *111*, D02308, doi:10.1029/2005JD006564.

Lobert, J., W. C. Keene, J. A. Logan, and R. Yevich (1999), Global chlorine emissions from biomass burning: Reactive Chlorine Emission Inventory, *J. Geophys. Res.*, *104*, 8373–8389.

Martin, R. V., et al. (2002), Interpretation of TOMS observations of tropical tropospheric ozone with a global model and in-situ observations, *J. Geophys. Res.*, *107*(D18), 4351, doi:10.1029/2001JD001480.

Mauzerall, D. L., J. A. Logan, D. J. Jacob, B. E. Anderson, D. R. Blake, J. D. Bradshaw, B. Heikes, G. W. Sachse, H. Singh, and B. Talbot (1998), Photochemistry in iomass burning plumes and implications for tropospheic ozone over the tropical South Atlantic, *J. Geophys. Res.*, *103*, 8401–8423.

Mauzerall, D. L., D. Narita, H. Akimoto, L. Horowitz, S. Walters, D. A. Hauglustaine, and G. Brasseur (2000), Seasonal characteristics of tropospheric ozone production and mixing ratios over East Asia: A global three-dimensional chemical transport model analysis, *J. Geophys. Res.*, *105*, 17,895–17,910.

McLinden, C. A., S. C. Olsen, B. Hannegan, O. Wild, M. J. Prather, and J. Sundet (2000), Stratospheric ozone in 3-D models: A simple chemistry and the cross-tropopause flux, *J. Geophys. Res.*, *105*, 14,653–14,665.

Osterman, G., et al. (2005), Tropospheric emission spectrometer (TES) validation report, version 1.00, JPL *D33192*, Jet Propul. Lab., Pasadena, Calif. (Available at http://tes.jpl.nasa.gov/docsLinks/documents.cfm)

Parrish, D. D., et al. (1993), Export of North America ozone pollution to the North Atlantic Ocean, *Science*, *259*, 1436–1439.

Parrish, D. D., M. Trainer, J. S. Holloway, J. E. Yee, M. S. Warshawsky, F. C. Fehsenfeld, G. L. Forbes, and J. L. Moody (1998), Relationships between ozone and carbon monoxide at surface sites in the North Atlantic region, *J. Geophys. Res.*, *103*, 13,357–13,376.

Rodgers, C. D. (2000), *Inverse Methods for Atmospheric Sounding: Theory and Practice*, World Sci., Hackensack, N. J.

Sarkissian, E., et al. (2005), TES radiometric assessment, *Eos Trans. AGU*, *86*(52), Fall Meet Suppl., Abstract A41A-0007.

Tan, W. W., M. A. Geller, S. Pawson, and A. da Silva (2004), A case study of excessive subtropical transport in the stratosphere of a data assimilation system, *J. Geophys. Res.*, *109*, D11102, doi:10.1029/2003JD004057.

Worden, J., S. S. Kulawik, M. W. Shephard, S. A. Clough, H. Worden, K. Bowman, and A. Goldman (2004), Predicted errors of tropospheric emission spectrometer nadir retrievals from spectral window selection, *J. Geophys. Res.*, *109*, D09308, doi:10.1029/2004JD004522.

M. A. Avery, Chemistry and Dynamics Branch, NASA Langley Research Center, Hampton, VA 23681, USA. (melody.a.avery@nasa.gov)

R. Beer, K. W. Bowman, A. Eldering, B. M. Fisher, S. S. Kulawik, Q. Li, H. M. Worden, and J. R. Worden, Jet Propulsion Laboratory, California Institute of Technology, 4800 Oak Grove Drive, Pasadena, CA 91109, USA. (reinhard.beer@jpl.nasa.gov; kevin.bowman@jpl.nasa.gov; annmarie.eldering@jpl.nasa.gov; brendan@tes-mail.jpl.nasa.gov; susan.s.kulawik@jpl.nasa.gov; qinbin.li@jpl.nasa.gov; helen.worden@jpl.nasa.gov; john.worden@jpl.nasa.gov)

R. C. Hudman, D. J. Jacob, J. A. Logan, and L. Zhang, Department of Earth and Planetary Sciences and Division of Engineering and Applied Sciences, Harvard University, Cambridge, MA 02138, USA. (hudman@fas.harvard.edu; djacob@fas.harvard.edu; jal@io.as.harvard.edu; linzhang@fas.harvard.edu)

M. C. Lampel, Raytheon Information Solutions, Pasadena, CA 91109, USA. (mlampel@sdsio-mail.jpl.nasa.gov)

C. P. Rinsland, NASA Langley Research Center, Mail Stop 401A, Hampton, VA 23681-2199, USA. (c.p.rinsland@larc.nasa.gov)

M. W. Shephard, Atmospheric and Environmental Research (AER), Inc., Lexington, MA 02421, USA. (mshephar@aer.com)

S. Turquety, Service d'Aéronomie, Institute Pierre-Simon Laplace, Université Pierre et Marie Curie, 4 place Jussieu, F-75252 Paris, France. (stu@aero.jussieu.fr)